Tensile And Formability Studies on AISI310 Austenitic Stainless Steel

Kosaraju Satyanarayana [1*], *Dharavath* Baloji [2], *Borrolla* Siddartha Reddy [1], *Kuduru* Rahul [1], *Mada Gowtham Sai* [1], *Murahari* Kolli[3], *M. Abdulfadhil* Gatea[4,5] *Harish Dutt* Sharma[6]

[1] Department Of Mechanical Engineering, Gokaraju Rangaraju Institute Of Engineering And Technology, Hyderabad 500090, India.
[2]Department Of Mechanical Engineering, KG Reddy College Of Engineering And Technology, Hyderabad 500072, India.
[3]Department of Mechanical Engineering, Lakireddy Bali reddy College of Engineering (A), Mylavaram, India.
[4] Technical Engineering Department College of Technical Engineering, The Islamic University, Najaf, Iraq
[5] Department of Physics, College of Science, University of Kufa
[6] Uttaranchal School of Computing Sciences, Uttaranchal University, Dehradun 248007 INDIA.

Abstract. Stainless steel is an alloy of iron, chromium, and, occasionally, nickel and other metals that resists corrosion. Metal is made into thin, flat pieces through an industrial process called sheet metal. One of the fundamental shapes used in metalworking, it can be cut and bent into many other shapes. Metal sheet is used to create a vast array of common items. The aim of the current work is to examine the 310 austenitic stainless steel's formability at room temperature with different strain rates (i.e 0.1&0.01mm/s). The study's outcomes were achieved through the utilization of the Nakazima test during stretch forming. Before performing formability test, The mechanical properties of a high-strength stainless steel AISI 310 were examined by conducting tensile tests at room temperature with 0.1,0.01mm/s strain rates. The failure modes, stress-strain curves of all the test specimens were obtained and analyzed.. In the current experiment, the stretch forming of different shaped metal was tested in servo electric hot forming machine with different strain rates i.e, (0.1,0.01) at room temperature and plotted forming limit diagrams based on the results. Then simulations of the experiments were performed in LS-dyna software and compared with the practical experiment results.

1.INTRODUCTION

[*]Stainless steel has numerous industrial and manufacturing applications due to its superior corrosion resistance when compared to conventional carbon steel, along with other benefits such as durability, ease of maintenance, and low life-cycle costs. These properties make it an

[*] Corresponding Author: satya.kosaraju@griet.ac.in

excellent choice for use industrial applications. However, due to its high cost, incomplete specifications, and design methods, stainless steel has mainly been utilized in maintenance structures and decorative components in the past few years. Nevertheless, with the increasing corrosion problems of steel structures, as well as higher demands for building use function and aesthetics, the advantages of stainless steel are increasingly being considered.

As a result, more researchers are studying stainless steel components, which support the improvement of the design method for stainless steel structures.[1]

Stainless steel and carbon steel exhibit different material characteristics at both room temperature and elevated temperature, primarily due to the high alloy content of stainless steel. At room temperature, stainless steel has a more rounded stress-strain response compared to carbon steel and does not have a well-defined yield point. Additionally, stainless steel has a higher ratio of ultimate-to-yield stress and greater ductility than carbon steel. When exposed to elevated temperatures, stainless steel maintains its strength and stiffness better than carbon steel. These properties make stainless steel ideal for use in structures under fire conditions. Austenitic stainless steel, in particular, has excellent strength, oxidation resistance, and room temperature as well as elevated temperature properties, making it a suitable choice for long-term, high-temperature industrial applications. This type of steel has been successfully used for such purposes for many years.[2]

Sheet metal forming is a manufacturing process that involves shaping thin, flat sheets of metal into three-dimensional objects using forces that do not significantly alter the thickness of the sheet. The process converts flat sheets into parts with the desired shape, achieved by applying forces that create stresses in the sheet and affect the thickness of the drawn part, which may vary in different parts of the object. Common sheet metal forming techniques, such as deep drawing, stretching, and bending, are used to produce a wide range of simple to complex components for various industrial applications.

Stretch forming is a crucial sheet metal forming process used in the production of sheet metal components for nuclear, automotive, aerospace, and domestic applications. In this process, a thin sheet metal blank is plastically deformed into the desired shape using forming tools, such as punches and dies, without fracturing. The success of the process depends on various factors, including the mechanical and metallurgical properties of the sheet metal, the geometry of the die and punch, the use of lubrication, the thickness of the sheet, the speed of the punch, and more. These factors are interdependent and contribute to the overall success of the forming process to varying degrees.

Having a comprehension of how easily sheet metals can be shaped is crucial for creating high-quality components. During the process of stretch forming, the sheet metal blank is subjected to various types of stresses, including tension (cup wall), bending (punch and die corners), and compression (cup flange). To be successful in stretch forming, the material must possess high tensile strength and good ductility in compression. The flange of the cup experiences radial tensile stresses from the pulling of the blank into the die cavity by the punch, as well as compressive hoop stresses due to the reduction in circumference. The flange may develop wrinkles due to compressive hoop stress. To prevent this from happening, the blank-holder is given sufficient force.[3] As the punch applies drawing force, the cup wall experiences longitudinal tensile stress. The punch action also creates tensile hoop stress in the flange. The depth of the flange that can be drawn is limited by the maximum tensile load

that the wall of the cup can bear, which is the highest force the punch can exert[4]. Drawing high strength metals at room temperature is challenging due to the substantial deformation and high flow stresses that the material experiences. However, drawing at elevated temperatures results in reduced flow stresses, relieves residual stresses, and makes deformation easier. Drawing at elevated temperatures enables deeper drawing and greater stretching in the final products.[5]

To develop new parts through forming, either through a single operation or several progressive ones, it's important to have accurate information about the achievable forming limits. In sheet metal forming, formability is restricted by the appearance of localized necking, so it's crucial to understand the material's forming limit. The formability of sheet metal is evaluated by examining the strain distribution during deformation and can be predicted through the forming limit diagram (FLD), which shows the different deformation paths of the material. The FLD reveals the correlation between the first principal strain (ε1) - which is the most significant in the plane of the sheet metal - and the second principal strain (ε2) - which is less significant in the plane of the sheet metal. The FLD provides a visual representation of sheet metal failure by mapping a forming limit curve (FLC), indicating the maximum strain a sheet metal can undergo without fracturing. The FLC is a limiting curve within the FLD, determining the maximum strain up to which a material can be formed before it fractures. The forming limit diagram (FLD) is a valuable tool for anticipating the formability of metal in sheet metal forming. It presents a visual representation of material failure during sheet metal forming processes. When the forming limit curve (FLC) is surpassed, the sheet experiences localized necking and fractures, which is known as the fracture zone. The safety curve is a parallel curve to the FLC, located 10% below it, and indicates a safe zone for strains that fall below it. The area between the FLC and safety curve is considered the critical strain region [6]. FLD is a commonly used method for presenting comprehensive information on formability. Materials that can distribute strains more evenly are located below the FLC and are expected to have greater formability. FLD enables the evaluation of various strain conditions on the same diagram and the determination of the fracture limit for particular strain combinations. Figure 1 depicts the diverse strain conditions in FLD, including various strain conditions in drawn cups represented in the same diagram. Fracture limits for formed cups differ depending on the specific strain combinations [7].The traditional forming of metals and alloys at room temperature can be challenging. Currently, research is being conducted to find ways to make this process easier.

Hussaini et.al,[8] Performed Using a hemispherical punch and stretching ASS 316 over a temperature range of RT to 400, an experimental FLD was plotted. They produced a theoretical FLD predicted by the Marciniak-Kuczynski model and compared it to an experimental FLD. Their research revealed that the FLD exhibited a predominance of major strain and that the dynamic strain ageing (DSA) onset was a crucial determinant of the metal's formability. Pavan Kumar et.al, [9] contrasted the results of several tests, including the Fukui's Conical Cup Drawing Test, the Swift Cu, and others, to determine the formability of steel and brass. Nejia Ayachi et.al, [10] The Nakazima test has been designed to assess the formability of thin copper sheets. The results of the test reveal that the Forming Limit Curves (FLCs) obtained using this method are comparable to those obtained through the reference Marciniak approach. Additionally, the data obtained through this test indicates a low value of major strain, which approaches a plane strain state. Nitin Kotkund et.al, [11] A Finite Element Analysis (FEA) was conducted on the Ti-6Al-4V alloy at a temperature of 400°C

for stretch forming. The DYNAFORM software, in conjunction with the LSDYNA server, was used for this purpose. The FEA results were then compared with the experimental data. The findings reveal that the yield criterion prediction by Barlat 1989 is more accurate than that of Hill 1948. Lumelskyj et.al, [12] Finite Element Analysis (FEA) was used to generate Forming Limit Curves (FLCs) for six specimens with varying widths (30, 50, 60, 77, and 99 mm) and a full circular specimen with a diameter of 110 mm. The specimens were divided into finite element meshes with an element size of h = 0.5 mm in the central region where failure was expected, and simulations were conducted using the Nakazima test model, with a constant punch velocity of 1 m/s. Based on the results, the authors concluded that comparing the numerical outcomes to the experimental FLC confirmed that it is feasible to utilize finite element simulations to determine FLCs

Sreenath et.al, [13] The FLD (Forming Limit Diagram) for AA2014 and AA2024 was created using the Nakazima test simulation tool. The experimental results were then compared with the simulation results, and the simulation tool was validated. The comparison showed a strong agreement between the FLCs generated through experimental means and software, indicating good agreement between the two. J.J.S. Dilip et.al, [14] During their investigation, the researchers observed that the consumable rods of alloy 2014-T6 had microstructures consisting of highly elongated grains containing a significant number of second-phase particles (ranging from 5 to 10 μm in size) that were aligned in the working direction. Analysis using SEM-EDS confirmed that these particles were Al2Cu and Fe-Mn-Al. In contrast, when examining the friction deposit in its as-deposited condition via SEM, very fine, equiaxed grains that were less than 3 μm in size were observed. The grain size was found to be consistent across the layers, indicating that reheating effects did not cause grain coarsening.

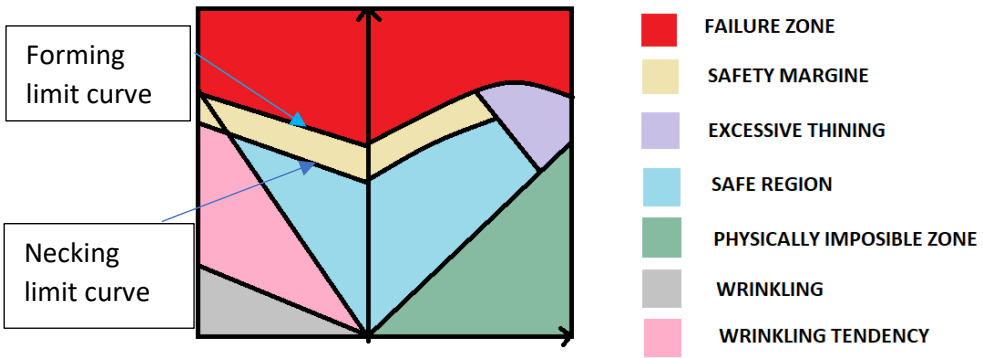

Fig. 1. Forming limit diagram

2. MATERIAL AND EXPERIMENTATION

The current study employs a 1.0 mm thick sheet of ASS 310 material. The chemical composition of ASS 310 sheet metal blank has been tested and is presented in Table 1.

Table 1: Chemical composition of AISI 310 sheet.

Element	Cr	Ni	C	Mn	Si	P	S	Fe
Composition (wt.%)	25	21	0.25	2	1.5	0.45	0.3	49.5

ASS stainless steel is an austenitic stainless steel with a high amount of chromium and nickel. It is considered a high-alloy steel due to its composition. It has excellent resistance to high temperatures and oxidation, and it is also known for its ability to withstand sulfidation and hot corrosion. It is resistant to scaling and corrosion at high temperatures due to its high nickel and chromium content.

This type of stainless steel is commonly used in high-temperature industrial applications where temperatures can exceed 800 degree celcius. Some of the applications where ASS 310 is used include heat exchangers, furnace parts, kiln linings, and other high temperature equipment. It also used in cryogenic applications because of its toughness and strength at low temperatures. The alloy can be formed using standard methods and is easily weldable.

Overall, ASS 310 is a versatile alloy that offers superior performance and properties in high-temperature and corrosive environments, making it a popular choice in various industrial applications.

2.1 Tensile test

To evaluate the mechanical properties of the AISI 310, Hot uni-axial Tensile test were conducted on the UTM with a heating frequency of 800-900 degree centigrade. According to the experimental parameters, project Matrix was designed and a total of 6 experiments were planned and carried out. The results were noted down from the inbuilt software. The fractured specimens were collected for the fractography studies of the material.

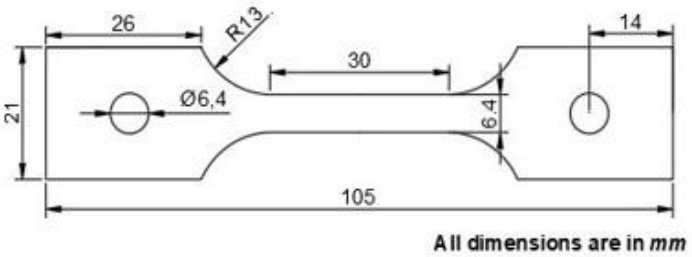

Fig. 2. ASTM-E8M tensile test standard specimen

Table 2. Design matrix

Std	Run	Temperature (°C)	Orientation	Strain rate (mm/sec)	YS (Mpa)	UTS (Mpa)	% of Elongation
1	1	Room temperature	0	0.1	265	463	45
2	2	Room temperature	45	0.1	254	456	43.5
3	3	Room temperature	90	0.1	244	448	42
4	4	Room temperature	0	0.01	258	458	43
5	5	Room temperature	45	0.01	244	454	41.2
6	6	Room temperature	90	0.01	229	447	40

2.3 Nakazima test

The study aimed to stretch the AISI310 material using a 20-ton hydraulic press equipped with a 2-zone split furnace and temperature controller that could maintain a consistent temperature with ±3% accuracy. The stretching apparatus comprised a 50mm diameter hemispherical dome-shaped punch and a blank holder plate with a grooved bead to restrict material flow into the cavity. The experiment involved using various Hasek specimens of different widths, and laser etching circular grids with a diameter of 5mm were done on the blanks to measure strains using a travelling electron microscope after the stretching operation. The experiment was carried out at room temperature with a punch speed of 0.1mm/s and two different strain rates (0.1, 0.01). Three different types of specimens were used to plot the forming limit diagram (FLD) in this study. The stretching setup was shown in Figure 2.

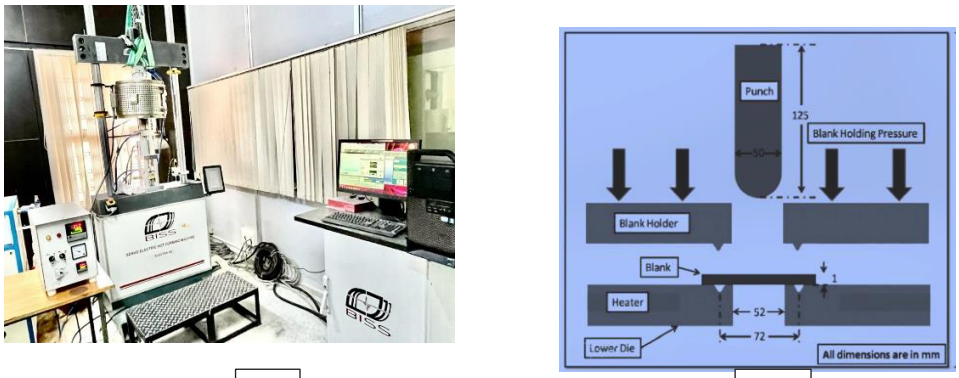

Fig. 3. A) Experimental setup B) Schematic diagram

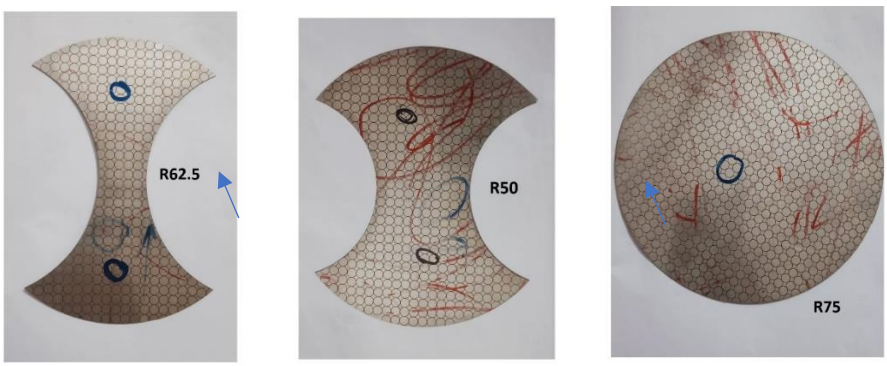

Fig. 4. Specimens for nakazima test A)R62.5 B)R50 C)75

3. Simulations

3.1 Mesh Formation and 3D Modelling:

In this study, the process of analyzing through FE (finite element) simulation involved creating models for the necessary tools and appropriately meshing them. The geometries of the tools and blank were created using SolidWorks and saved in STEP File format. These meshes were then imported into LS-Dyna. Once the meshing was complete, the initial and boundary conditions, as well as process parameters, were defined. The blank was designated as the deformable body, while the other tools were considered rigid bodies.

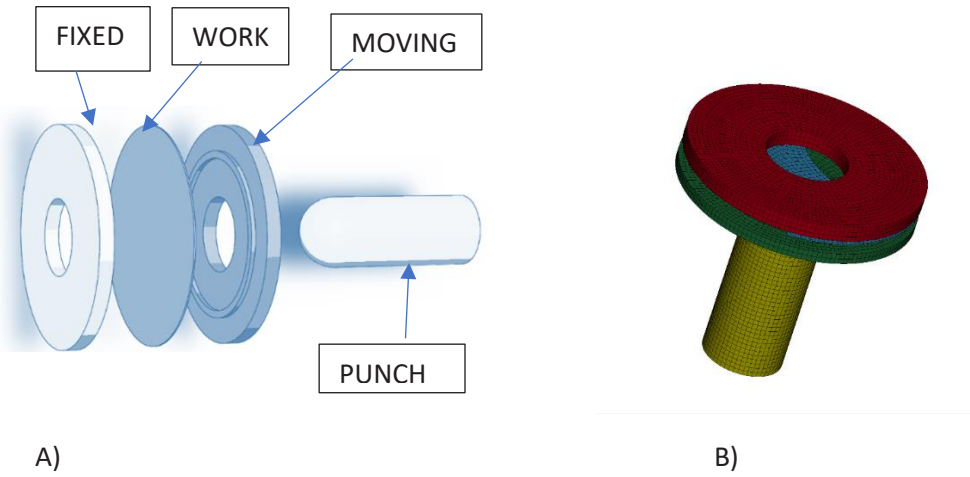

Fig. 5. A) 3D model for stretch forming B) Finite element model

3.2 Simulations on finite elements

Finite Element Analysis (FEA) is a method used to simulate and investigate how materials and structures behave when subjected to different loading conditions. It involves breaking down the structure or material into smaller and simpler parts known as finite elements and solving the equations that dictate the behaviour of each element. The results of these equations can be used to predict how the material or structure as a whole will behave when subjected to different types of loading. FEA simulations are particularly useful for analysing complex materials or structures such as stainless steel aisi310, where analytical methods are insufficient. These simulations can model a wide range of physical phenomena, including deformation, stress, strain, and thermal behaviour. By combining the results of each individual component, an overall performance of the material or structure can be predicted. This approach can provide valuable insights into how the material or structure will react to various types of stress, such as changes in strain rate, alterations in pressure, or mechanical strains. Table 2 and Table 3 display the material properties and process parameters obtained from the simulations.

Table 3: properties used for simulations

Yield strength (MPa)	Failure criteria	Elastic modulus (MPa)	r	N	Poisson's ratio (pr)	Mass density (kg/m^3)
252.23000	1.56	19444	0.285	0.121	0.29	7750

Table 4: process parameters

Diameter of hemispherical dome-shaped punch:	50mm
Blank material:	AISI310
Blank thickness:	1mm
Fixed and moved Plate Diameter:	150mm
Type of contact:	Forming one way surface to surface
Element type:	Rectangular and triangular
Blank element size:	3mm

The method for selecting measurement elements is as follows:

- The elements located in the necking area are chosen randomly.
- The occurrence of a localized necking state is confirmed by examining the true stress value, which corresponds to the Ultimate Tensile Stress value of the material.
- If necking is not observed, the simulation is continued until the equivalent stress value exceeds the true stress value corresponding to the ultimate tensile stress.

4. Results

4.1 Tensile test

From the experiments conducted on the AISI 310 results shows that mechanical properties are varying with the experimental parameters. As the experimental stain rate is increased the UTS, YS, % of elongation of the material started to increase simultaneously. As the temperature is kept constant it did not keep affecting on the mechanical properties of the metal. Initially the atoms of the material where stable it requires some heat which means of temperature in order to dislocate the atoms and make strength of the material to low, as we are not taking temperature to our consideration the temperature did not show any much effect on the mechanical properties. As the strain increased simultaneously mechanical properties also increased due to the atoms inside the material will be in stable condition initially as the strain is increased the atoms will pile up as the strain is increased the atoms starts to prevent the further breaking of the bonds between with atoms. As the more and more strain is increased more and more strength starts to accumulate on the atoms as the strength and elongation of the material also starts to increase.

The mechanical properties of the material are observed to be high in the 0-degree specimen sample compared to the other orientation samples.

The maximum UTS is observed to be the 263mpa at 0.1mm/sec strain rate for the 0-degree specimen and minimum UTS is observed to be 258mpa at 0.01mm/sec strain rate for the 0-degree specimen sample. The maximum YS is observed to be the 262mpa at 0.1mm/sec strain rate for the 0-degree specimen and minimum YS is observed to be 258mpa at 0.01mm/sec strain rate for the 0-degree specimen sample. The maximum % of elongation is observed to be the 45% at 0.1mm/sec strain rate for the 0-degree specimen and minimum % of elongation is observed to be 43% at 0.01mm/sec strain rate for the 0-degree specimen sample.

4.2. Factrography studies

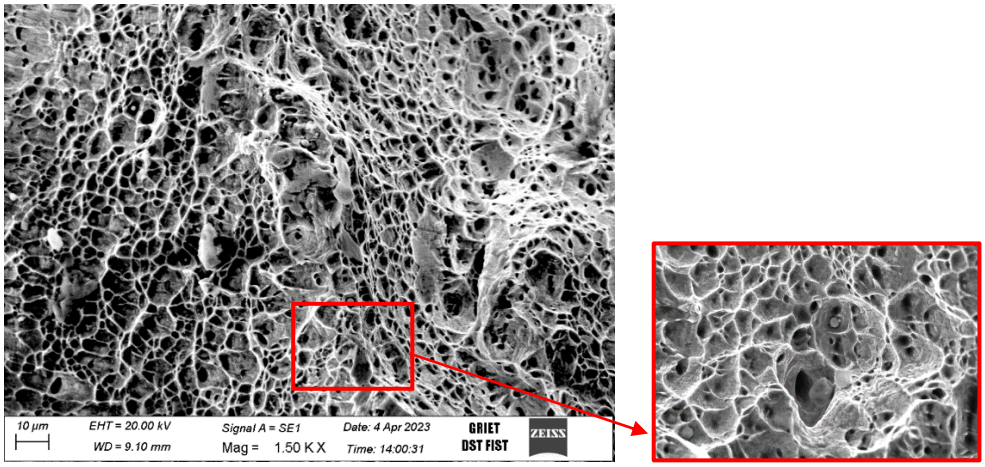

Fig. 6. Microstructure of tensile sample

The SEM (Scanning Electron Microscope) views of AISI310 deformed specimens at maximum mechanical properties (Room temperature at 0.1 mm/sec strain rate specimen for the max percent of elongation, room temperature at 0.1mm/sec strain rate specimen for the max UTS value and room temperature at 0.1mm/sec strain rate specimen for the max YS value) were observed and shown in fig6. The presence of voids, dimples on the fracture surface were observed.

4.3 Forming limit diagram

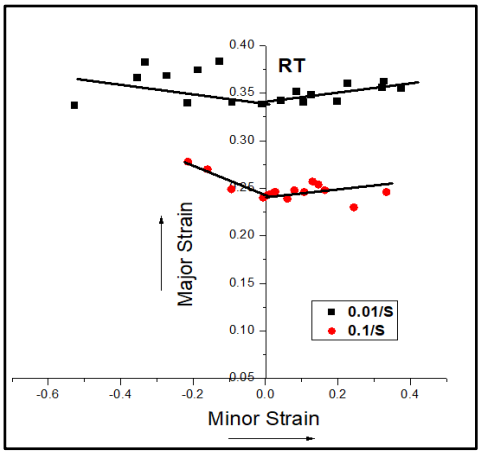

Fig. 7. Forming limit diagram for room temperature with two strain rates (0.1,0.01)

The above figures show the effect of strain rate on the ability of ASS 310 to undergo deformation at room temperature. The forming limit diagram (FLD) is used to represent the range of safe deformation below the curve. It can be observed from the figures that the impact of strain rate on the FLD is significant, especially at 0.01/s, indicating that it has a dominant effect. Moreover, the FLD slightly shifts upwards from 0.1/s to 0.01/s. As the minor strain

gradually increases, the gap between the curves narrows, implying that the blank is safer at lower minor strain levels.

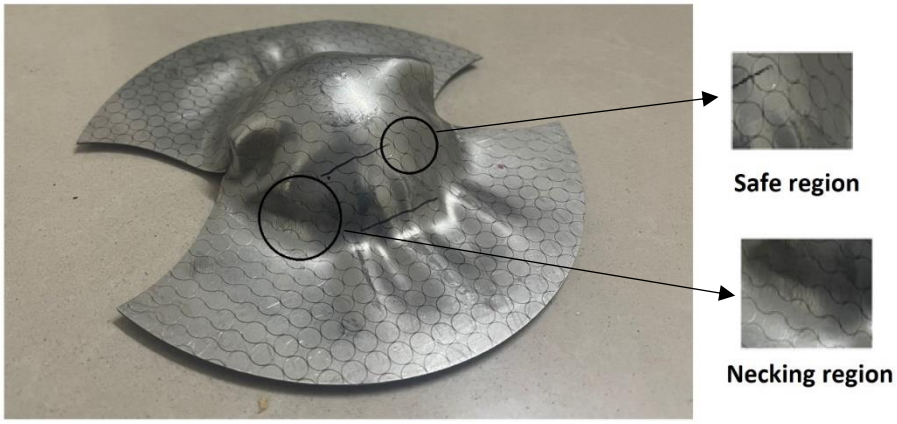

Fig. 8. Necking, Safe regions of the Dome-Shaped specimen

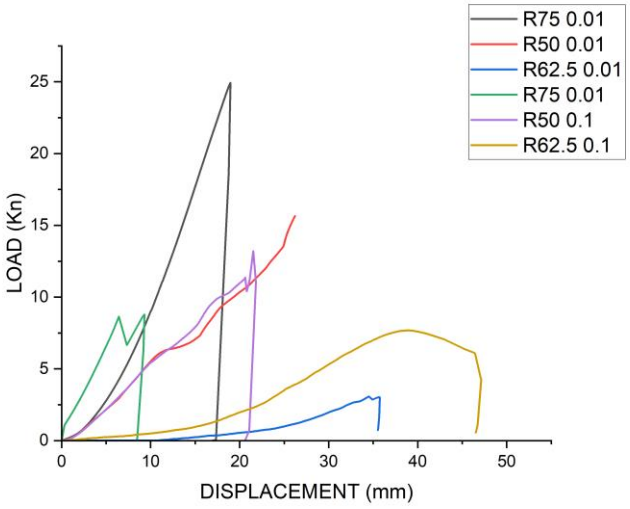

Fig. 9. Load vs displacement graph

4.4 Analysis of AISI310

The aim of this study is to establish a connection between the limit strains predicted by finite element simulations and the limit strains obtained through experiments. The research involved the simulation of three different specimens under various tension states at room temperature, which produced specific points on the forming limit diagram (FLD). Table 4 presents the major and minor strains acquired from both simulations and experiments. The minor and major strains of each element were documented based on the selection criteria discussed earlier.

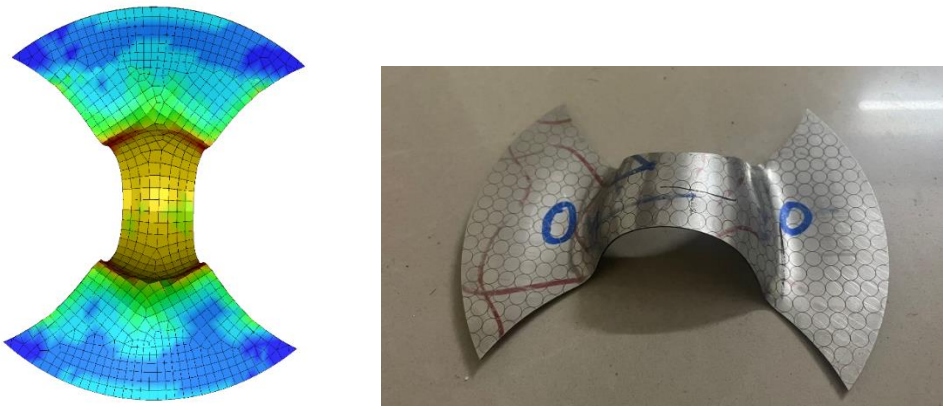

Fig. 10. Comparison between experimental sample and simulation result.

LS Dyna finite element software was utilized to simulate the Nakazima test for specimens made of AISI 310, and the measuring elements were selected following the previously established criteria. The major and minor strain values of the elements were collected and plotted on a Forming Limit Curve (FLC) graph to determine the FLC of AISI 310.

Table 5. Experimental and simulation results

Specimen Dimensions (mm)	**Experimental values**		**Simulation Results**	
	Major Strain	**Minor Strain**	**Major strain**	**Minor Strain**
R75	0.123	0.12	0.19	0.18
R62.5	0.0688	-0.221	0.0799	-0.332
R50	0.093	-0.434	0.125	-0.586

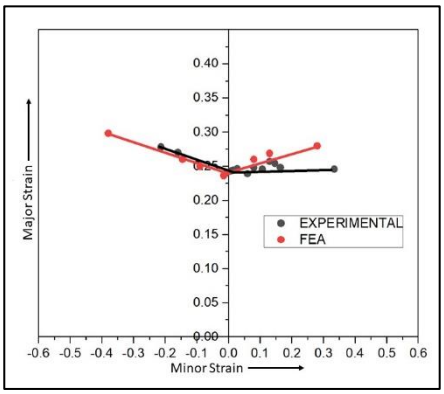

FIG.11. FLD generated by experiment and FEA

The experimental and software-generated Forming Limit Curves (FLCs) exhibit a high degree of agreement with minimal discrepancies, indicating that the results obtained from experiments are significant.

The simulations provided results on von Mises stress, effective plastic deformation, and resultant deformation. Von Mises stress, also known as equivalent or distortion energy stress, is a way of determining the maximum stress a material can handle before experiencing plastic deformation. It takes into account both normal and shear stresses acting on the material and is calculated based on the three-dimensional stress tensor. This stress measurement is an effective tool for predicting material failure and designing structures capable of withstanding anticipated loads.

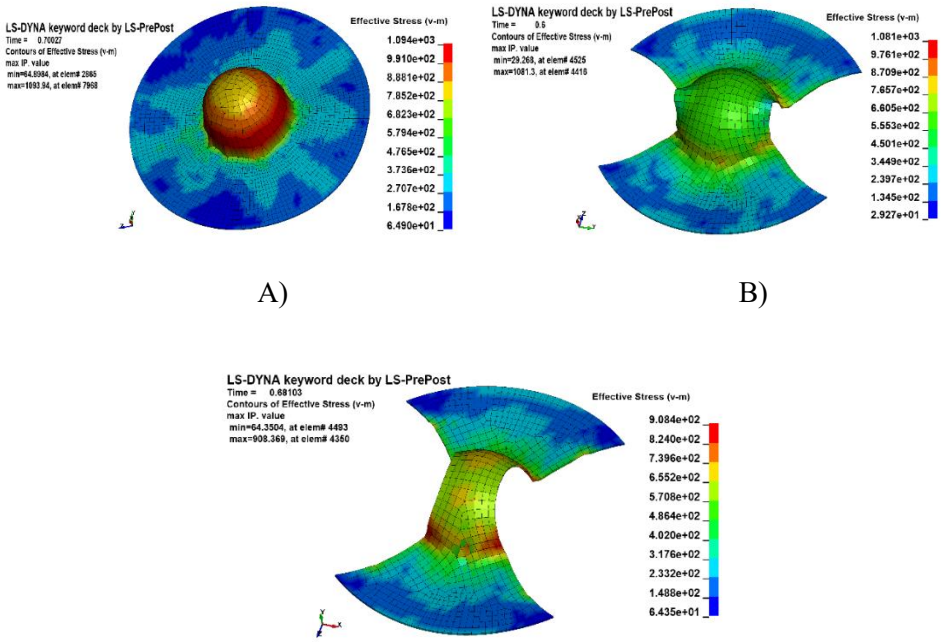

Fig. 12. Simulations results of effective stress a)R75; b)R50; c) R62.5

The analysis indicated that the R75 geometry had the highest effective stress, as demonstrated in Figure 10. The region where the punch comes into contact with the specimen experiences the highest effective stress, while the non-forming region experiences the lowest. The effective stress increases with deformation until the point of fracture is reached.

Effective plastic strain is a metric that measures the plastic deformation that a material undergoes when subjected to mechanical loading. It is distinct from total plastic strain, which considers all plastic deformation that occurs throughout the

material, as effective plastic strain only measures the plastic deformation in regions where the material has yielded beyond its elastic limit. This parameter is crucial in determining the material's behavior under load, as it can be used to predict factors such as material failure, fatigue, and overall durability. Engineers and scientists use various testing methods, such as tensile and compression tests, to assess effective plastic strain, which helps them understand how materials behave under stress and design more resilient structures and products. The permanent deformation caused by pushing the material beyond its elastic limit is considered an effective plastic strain.

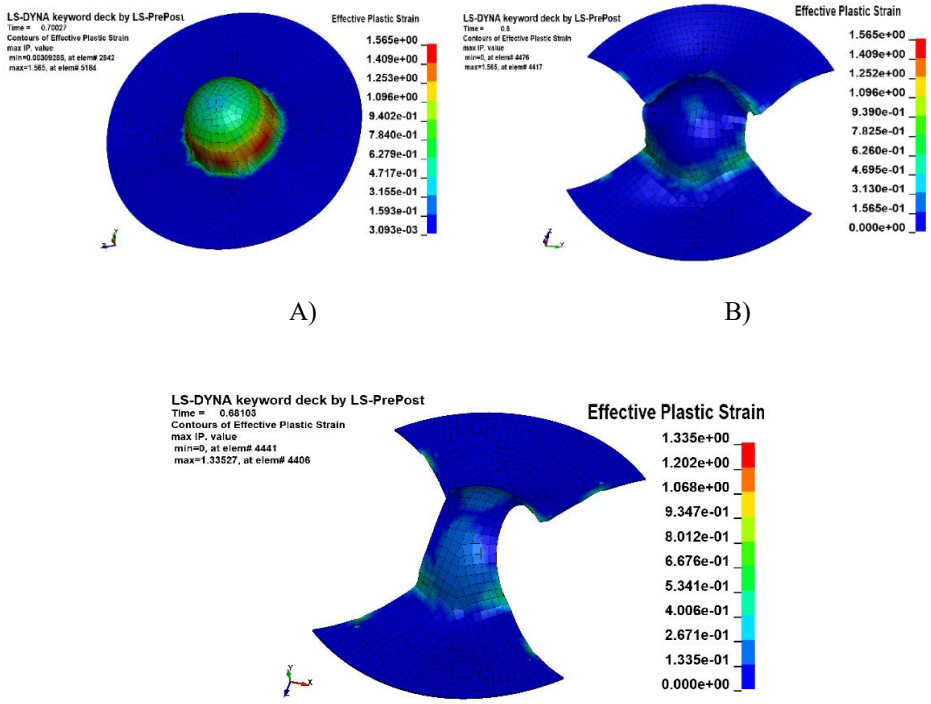

Fig. 13. Simulations results of effective plastic strain a)R75; b)R50; c)R62.5

According to the simulation results displayed in Figure 11, it was observed that the R62.5 geometry produced the highest effective plastic strain (EPS), and the maximum EPS value for R50 and R75 was found at the center of the geometry. In the case of the R62.5 shape, the maximin EPS was found at the edges of the dome shape. Additionally, it was observed that an increase in deformation resulted in an increase in EPS.

The resultant displacement in finite element analysis refers to the total displacement of a structure or element resulting from applied loads or given time. It is calculated by solving a set of equations that depict the structure's behaviour under specific loading circumstances. The magnitude and direction of the resultant displacement can be determined and used to evaluate the overall deformation and stability of the structure. Precise computation of the resultant displacement is essential in engineering design to ensure that the structure can

withstand intended loads and remain intact over time. Finite element analysis software is commonly used to perform these calculations and can provide detailed information on the behavior of complex structures under various loading scenarios.

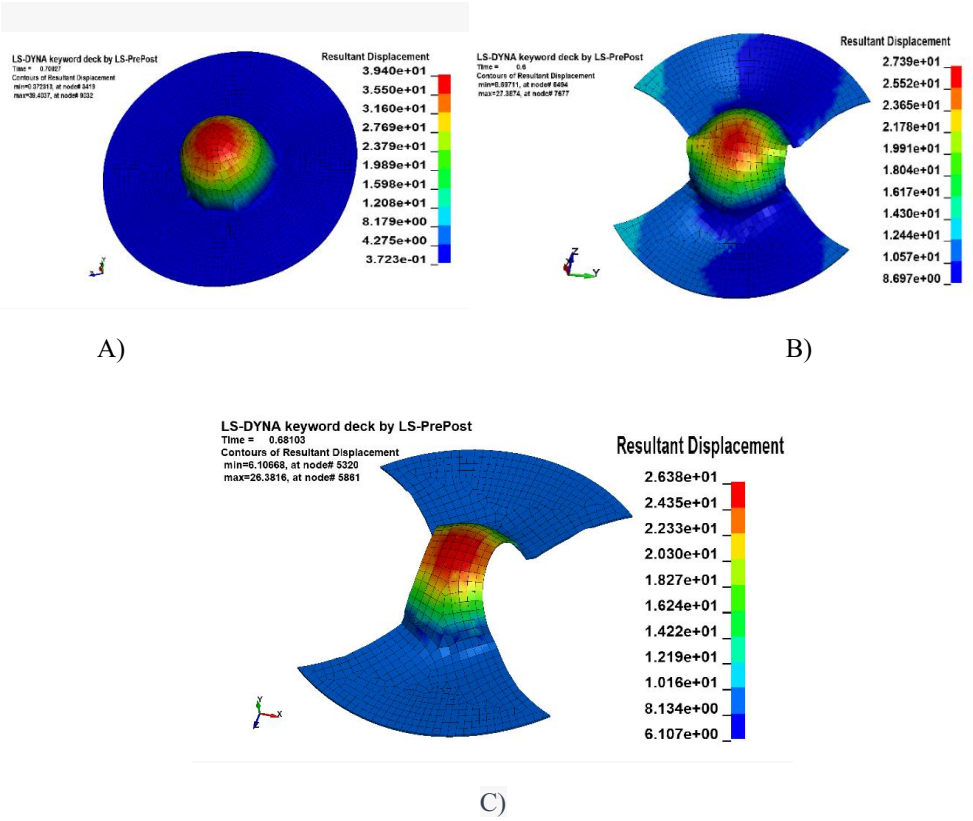

Fig. 14. Simulations results of resultant displacement a)R75; b)R50; c)R62.5

The punch displacement for the R62.5 specimen was found to be greater, reaching 26.3mm, as shown in figure 12. This is due to the particular shape of the specimen, which causes an increase in stress as the punch displacement increases. Both simulation and experimental results indicate similar punch displacement values.

5.CONCLUSION

5.1 Tensile test

An attempt was made to investigate the mechanical properties of the AISI310 was made and the conclusions were stated as follows:

- As the strain rate is increased the mechanical properties of the material started to increase.

- For the 90-degree specimen the mechanical properties of the materials were maximum.
- Compared to orientation the strain rate played a key role in the mechanical properties of the material.

5.2 Formability test

The aim of this study was to determine the forming limits at room temperature through both experimental and finite element simulations. The study has yielded several important results, which are summarized below.

- The forming behavior of AISI 310 was studied through the Nakajima test with varying strain rates (0.1, 0.01) at room temperature.
- An experimental Forming Limit Diagram (FLD) for AISI 310 at room temperature was established with different strain rates.
- The FLD generated through LS dyna simulation was compared with the experimental FLD at room temperature, and showed minimal error.
- It was observed that drawing AISI 310 was challenging at a strain rate 0.01, and the Limiting Drawing Height (LDH) increased as the strain rate increased.
- Necking was observed in dome-shaped cups during the study.

REFERENCES

1. Andrea Di Schino, Manufacturing and Applications of Stainless Steels, 1 March 2020
2. Gardner, L., Insausti, A., Ng, K. T. and Ashraf, M. (2010). Elevated temperature material properties of stainless steel alloys. Journal of Constructional Steel Research. 66(5), 634-647.
3. Syed Mujahed Hussaini, Geetha Krishna, Amit Kumar Gupta, Swadesh Kumar Singh, Development of experimental and theoretical forming limit diagrams for warm forming of austenitic stainless steel 316, Journal of Manufacturing Processes, Volume 18, April 2015.
4. Tummala, S.K., Indira Priyadarshini, T., Morphological Operations and Histogram Analysis of SEM Images using Python, Indian Journal of Engineering and Materials Sciences, 2022, 29(6), pp. 794–798.
5. Swadesh Kumar Singh , K. Mahesh , Apurv Kumar , M. Swathi Understanding formability of extra-deep drawing steel at elevated temperature using finite element simulation, 29 April 2010.
6. Mitsutoshi Kuroda*, 1, Viggo Tvergaard , Forming limit diagrams for anisotropic metal sheets with different yield criteria 16 July 1999.
7. Baloji Dharavath, Ayush Morchhale, Nitin Kotkunde, Swadesh Singh, Experimental Determination and Theoretical Prediction of Limiting Strains for ASS 316L at Hot Forming Conditions, Journal of Materials Engineering and Performance, Volume 29, July 2020.
8. Suresh Kumar Tummala, Phaneendra Babu Bobba & Kosaraju Satyanarayana (2022) SEM & EDAX analysis of super capacitor, Advances in Materials and Processing Technologies, 8:sup4, 2398-2409

9. Syed Mujahed Hussaini, Geetha Krishna, Amit Kumar Gupta, Swadesh Kumar Singh, Development of experimental and theoretical forming limit diagrams for warm forming of austenitic stainless steel 316, Journal of Manufacturing Processes, Volume 18, April 2015.
10. J Pavan Kumar, R Uday Kumar, B Ramakrishna, B Ramu and K Baba Saheb 2nd International Conference on Advancements in Aeromechanical Materials for Manufacturing, volume 455,july 2018.
11. Davu, S.R., Tejavathu, R. & Tummala, S.K. EDAX analysis of poly crystalline solar cell with silicon nitride coating. Int J Interact Des Manuf (2022).
12. B. J. Varghese, P. B. Bobba and M. Kavitha, "Effects of coil misalignment in a four coil implantable wireless power transfer system," 2016 IEEE 7th Power India International Conference (PIICON), Bikaner, India, 2016, pp. 1-6
13. Nejia Ayachi , Noamen Guermazi , Cong Hanh Pham . Development of a Nakazima Test Suitable for Determining the Formability of Ultra-Thin Copper Sheets, Metals 2020, 10(9), 116, august 2020.
14. B. J. Varghese and P. B. Bobba, "Design and analysis of a robust system for wirelessly powering implantable devices," 2016 IEEE 1st International Conference on Power Electronics, Intelligent Control and Energy Systems (ICPEICES), Delhi, India, 2016, pp. 1-5
15. Nitin Kotkunde , Amit Kumar Gupta a, Prudvi Reddy Paresi , Swadesh Kumar Singh, Experimental and Finite Element Studies of Stretch Forming Process for Ti-6Al-4V Alloy at Elevated Temperature, Materials Today: Proceedings Volume 4, Issue 4, 2017.
16. M. Kavitha, P. B. Bobba and D. Prasad, "Effect of coil geometry and shielding on wireless power transfer system," 2016 IEEE 7th Power India International Conference (PIICON), Bikaner, India, 2016, pp. 1-6
17. Lumelskyj a, J. Rojek a, L. Lazarescu b, D. Banabic b, Determination of forming limit curve by finite element method simulations. Procedia Manufacturing, Volume 27, 2019,
18. Sreenath D Kumar, Amjith T.R, C. Anjaneyulu, Forming Limit Diagram Generation of Aluminium Alloy AA2014 Using Nakazima Test Simulation Tool, Procedia Technology, Volume 24, 2016.
19. Karthik Rao, R., Bobba, P.B., Suresh Kumar, T., Kosaraju, S., Feasibility analysis of different conducting and insulation materials used in laminated busbars, Materials Today: Proceedings, 2019, 26, pp. 3085–3089.
20. J.J.S. Dilip, G.D. Janaki Ram, Microstructure evolution in aluminium alloy AA 2014 during multi-layer friction deposition, Materials Characterization, volume 86, December 2013
21. Prasad, K.S., Gupta, A.K., Singh, Y., Singh, S.K., A Modified Mechanical Threshold Stress Constitutive Model for Austenitic Stainless Steels, Journal of Materials Engineering and Performance, 2016, 25(12), pp. 5411–5423
22. Singh, S.K., Tambe, S.P., Raja, V.S., Kumar, D., Thermally sprayable polyethylene coatings for marine environment, Progress in Organic Coatings, 2007, 60(3), pp. 186–193.
23. Naik, R.B., Ratna, D., Singh, S.K., Synthesis and characterization of novel hyperbranched alkyd and isocyanate trimer based high solid polyurethane coatings, Progress in Organic Coatings, 2014, 77(2), pp. 369–379
24. Sandeep Pandre, Ayush Morchhale, Nitin Kotkunde & Swadesh Kumar Singh (2020) Influence of processing temperature on formability of thin-rolled DP590 steel sheet, Materials and Manufacturing Processes, 35:8, 901-909.